

# Temporal dynamics of microbial communities in microcosms in response to pollutants

SHUO JIAO,\* ZHENGQING ZHANG,† FAN YANG,\* YANBING LIN,\* WEIMIN CHEN\* and GEHONG WEI\*

\*State Key Laboratory of Crop Stress Biology in Arid Areas, College of Life Sciences, Northwest A&F University, Yangling, Shaanxi 712100, China, †Laboratory of Forestry Pests Biological Control, College of Forestry, Northwest A&F University, Yangling, Shaanxi 712100, China

## Abstract

Elucidating the mechanisms underlying microbial succession is a major goal of microbial ecology research. Given the increasing human pressure on the environment and natural resources, responses to the repeated introduction of organic and inorganic pollutants are of particular interest. To investigate the temporal dynamics of microbial communities in response to pollutants, we analysed the microbial community structure in batch microcosms that were inoculated with soil bacteria following exposure to individual or combined pollutants (phenanthrene, *n*-octadecane, phenanthrene + *n*-octadecane and phenanthrene + *n*-octadecane + CdCl<sub>2</sub>). Subculturing was performed at 10-day intervals, followed by high-throughput sequencing of 16S rRNA genes. The dynamics of microbial communities in response to different pollutants alone and in combination displayed similar patterns during enrichment. Specifically, the *repression* and *induction* of microbial taxa were dominant, and the *fluctuation* was not significant. The rate of appearance for new taxa and the temporal turnover within microbial communities were higher than the rates reported in other studies of microbial communities in air, water and soil samples. In addition, conditionally rare taxa that were specific to the treatments exhibited higher betweenness centrality values in the co-occurrence network, indicating a strong influence on other interactions in the community. These results suggest that the repeated introduction of pollutants could accelerate microbial succession in microcosms, resulting in the rapid re-equilibration of microbial communities.

**Keywords:** conditionally rare taxa, environmental pollution, microbial succession, microcosm, temporal dynamics

Received 8 August 2016; accepted 8 December 2016

## Introduction

In ecology, succession refers to the dynamic changes that take place in the abundance and composition of species in a given community over time; understanding this process is a major goal of ecological research (Shade *et al.* 2013). Studies on the succession of microbial communities in response to environmental changes are increasing due to the important ecological functions

of microbes (Fierer *et al.* 2010). Although surveying microbial succession is challenging, high-throughput sequencing and other culture-independent approaches have accelerated progress, because these methods can detect most of the microbial taxa that are present in a given sample (Gonzalez *et al.* 2012).

Microbial succession has been explored in many diverse systems, including primary succession in the infant gut (Koenig *et al.* 2011), recurring seasonality in aquatic systems (Eiler *et al.* 2012; Gilbert *et al.* 2012), re-treating glacier soils (Brown & Jumpponen 2014) and environments polluted with heavy metals (Hur *et al.* 2011) or petroleum (Mikkonen *et al.* 2011; Yu

Correspondence: Gehong Wei and Weimin Chen, Fax: +86 29 87091175, +86 29 87091175; and E-mails: weigehong@nwsuaf.edu.cn, chenwm029@nwsuaf.edu.cn

*et al.* 2011). A recent meta-analysis revealed that temporal variability in microbial communities is consistent among similar environments (Shade *et al.* 2013). Because the temporal dynamics of microbial communities in natural environments are influenced by multiple environmental factors simultaneously, it is difficult to determine the relative contributions made by individual factors to the overall microbial succession process (Jiao *et al.* 2016). Microcosms can serve as models of closed systems with tightly controlled conditions, facilitating the investigation of temporal dynamics in microbial communities that occur following changes in single environmental factors (Viñas *et al.* 2005).

A vital indicator for the dynamics of microbial succession is the temporal turnover of the time–decay relationship (TDR), which has been used to describe decreasing community similarities over time (Nekola & White 1999). Community temporal turnover is the elimination and replacement of species over time, as applied to studies on animal and plant communities (Hatosy *et al.* 2013; MacArthur & Wilson 2015). Microbial communities in the air, water and soil also exhibit similar temporal patterns with significant TDRs (Shade *et al.* 2013). Additionally, community temporal dynamics can be estimated by the species–time relationship (STR), the temporal analog of the widely used species–area relationship. STRs are primarily focused on changes in alpha diversity and species richness over time (Preston 1960; Rosenzweig 1995). Significant STRs have been reported for microbes on leaf surfaces (Redford & Fierer 2009), in bioreactors (van der Gast *et al.* 2008) and in soils (Shade *et al.* 2013), suggesting that they are generally applicable to the microbial communities in different environments.

Highly diverse and complex microbial communities are present in all ecosystems, where they play crucial roles in biogeochemical processes (Falkowski *et al.* 2008). Interestingly, microorganisms that are present at low levels may contribute to the function and stability of ecosystems (Shade *et al.* 2014), as suggested for diazotrophs in seawater (LaRoche & Breitbart 2005), archaeal ammonia oxidizers in soils (Leininger *et al.* 2006) and methanogens in the gut (Horz & Conrads 2010). When environmental conditions are altered, these rare microorganisms may become locally extinct, or they may be maintained at low levels or become more abundant and able to play a greater role in a given ecosystem. Shade *et al.* (2014) defined conditionally rare taxa (CRT) as microbial taxa that are usually present at low levels within a community, but they may become abundant under particular conditions. Although CRT contribute greatly to temporal community dissimilarity (Shade *et al.* 2014), their ecological roles and functional

importance in habitats exposed to complex pollutants remain unknown.

In the present study, we investigated the composition of microbial communities that were exposed to two organic pollutants (the aliphatic alkane *n*-octadecane and the aromatic phenanthrene) separately and in combination, in both the presence and the absence of cadmium, using high-throughput sequencing of 16S rRNA genes. To ensure that succession was caused by the pollutants, tightly regulated microcosms were used as a simple model for understanding the complex interactions between environmental factors and microbial communities. The ultimate objective of this study was to investigate succession in microbial communities in response to the pollutants.

## Materials and methods

### Sampling site

Contaminated surface soil (0–30 cm depth) was collected from a 100 × 100 m<sup>2</sup> area surrounding an oil refinery (E 108°50'10" and N 37°35'35") in Yulin City, northwest China. This area has been contaminated continuously with crude oil over the last 20 years, and no plants grow there. Five soil cores (~5 cm in diameter) were removed from the sampling area using the cross-technique (samples were collected from the four corners and the centre), placed in sterile plastic bags and immediately transported to the laboratory on dry ice. A portion of each soil sample was air-dried to analyse the edaphic properties. The remaining sample portions were stored at 4 °C in a sealed plastic bag until needed and were then used within 1 week in all cases. The soil was of a sandy loam texture and contained total petroleum hydrocarbons of 5.69 ± 0.01 g/kg of dry soil, as measured using the ultrasonic-Soxhlet extraction gravimetric method (Huesemann 1995). The pH was 7.7, and the other parameters were as follows: available nitrogen, 38.0 mg/kg; total nitrogen, 2776.3 mg/kg; available potassium, 87.5 mg/kg; available phosphorus, 52.1 mg/kg; total phosphorus, 989.2 mg/kg; organic matter, 6.9 g/kg; cation-exchange capacity, 8.6 cmol/kg; and water-holding capacity, 22.4%.

### Preparation of microcosms

Microcosms were constructed using basal salt medium (BSM; Jiao *et al.* 2016) supplemented with (i) 500 mg/L phenanthrene (PHE), (ii) 500 mg/L *n*-octadecane (C18), (iii) 250 mg/L phenanthrene + 250 mg/L *n*-octadecane (PC) or (iv) 250 mg/L phenanthrene + 250 mg/L *n*-octadecane + 50 mg/L CdCl<sub>2</sub> (PCC). Both phenanthrene and *n*-octadecane are components of petroleum

and can be used as a carbon source by bacteria. Cadmium (Cd) was used because it is a heavy metal that is highly toxic to animals, plants and microorganisms (Thavamani *et al.* 2012). To prepare the BSM + pollutants, organic pollutants were dissolved in dichloromethane, placed in an empty sterile flask and mixed with BSM after solvent evaporation (Jiao *et al.* 2016). For the PCC, the dissolved CdCl<sub>2</sub> was added to an empty flask, and organic pollutants were added after autoclaving.

At the beginning of the enrichment process, 20 g of contaminated soil was added to 180 mL of sterilized NaCl solution (0.85%). After being shaken for 10 min at 240 rpm, 20 mL of supernatant from the soil suspension was used to inoculate 180 mL of BSM supplemented with the appropriate pollutant. The effects of the initial soil properties on the microcosms were neglected as the soil was diluted more than 100-fold, and only the supernatant was used as the inoculum. All of the treatments were performed in triplicate. Inoculated microcosms were incubated at 28 °C with shaking (150 rpm) in the dark to avoid pollutant photolysis. Successive subcultures were grown at 10-day intervals over a 100-day incubation period. According to our previous study (Jiao *et al.* 2016), the 10-stage enrichment process could be divided into three phases as follows: I (subcultures 1–3), II (subcultures 4–7), and III (subcultures 8–10), and these categories were used in all of the subsequent analyses. The biomass from each subculture was collected by centrifugation at 10 000 g for 15 min at room temperature for microbial analysis and was stored at –80 °C for subsequent DNA extraction. All of the operations were performed under aseptic conditions.

#### *Analysis of residual organic pollutants*

The residual organic pollutants were extracted from supernatants with an equal volume of dichloromethane. The pollutant concentration was determined by gas chromatography with flame ionization detection (Model GC-2010 plus; Shimadzu, Kyoto, Japan) using an SE30 capillary column (30 m long, 0.25 mm inside diameter, 0.25 mm film thickness) with helium as a carrier gas. The initial oven temperature was 80 °C, and heating was conducted at a rate of 50 °C/min to 200 °C, where it was held for 1 min, then heated to 210 °C at a rate of 1 °C/min. The temperature of the injector and detector was 290 °C. The total helium flow rate was 30.0 mL/min, and the column flow rate was 30.0 mL/min. The components were identified by matching their retention times with authentic standards. The biodegradation efficiency was calculated as the ratio of the pollutant concentrations in blank controls to treatments.

#### *DNA preparation and MiSeq sequencing*

Metagenomic DNA was extracted from the initial soil sample using a FastDNA SPIN Kit for Soil (MP Biochemicals, Solon, OH, USA) and from the microcosms (treatments) using the sodium dodecyl sulphate–cetyltrimethylammonium bromide (SDS–CTAB) method (Wilson 1987). The microbial communities were profiled by targeting the V4–V5 hypervariable regions of the 16S rRNA gene (Yu *et al.* 2015) using the Illumina MiSeq (250-bp paired-end reads) platform at Macrogen Inc. (Seoul, South Korea; <http://www.macrogen.com>) as described previously (Jiao *et al.* 2016).

#### *Data analysis*

Prior to data analysis, a subsample with a minimum of 15 925 sequences (according to the sample size) from each sample was used to eliminate all potential inaccuracies. Sequences with  $\geq 97\%$  similarity were assigned to the same operational taxonomic units (OTUs). Multiple indices (Chao1 richness, observed OTUs, Pielou's evenness, Shannon's index and Simpson's index) were calculated using the QIIME package (<http://qiime.org/index.html>) to present the alpha diversity; pairwise weighted UniFrac and Bray–Curtis dissimilarities were estimated between the samples. A constrained analysis of principal coordinates (CAP) was performed to evaluate the relationship between the treatments and bacterial community composition. A principal coordinate analysis was performed on distance matrices to visualize the sample relationships, and a canonical discriminant analysis (CDA) was used to identify the taxa associated with different treatments. A similarity analysis (ANOSIM; Clarke 1993) and a permutational multivariate analysis of variance (ADONIS; Anderson 2001) were performed to determine whether the sample classifications (different treatments) contained significant differences in phylogenetic or species diversity based on weighted UniFrac and Bray–Curtis dissimilarity matrices.

The association strength (correlation coefficient, *R*) of each OTU to the treatment was determined using a correlation-based indicator species analysis (Cáceres & Legendre 2009) with 10<sup>3</sup> permutations. *P*-value adjustments for multiple comparisons were performed using the false discovery rate (FDR) correction according to Storey (2002), and associations were considered significant at  $q < 0.05$ . Bipartite networks were generated in CYTOSCAPE (Smoot *et al.* 2011) using treatments as source nodes and indicator OTUs as target nodes, with edges (the lines connecting the nodes) representing positive associations between indicator OTUs and treatments.

The dynamic patterns in microbial taxa during enrichment (subculture) were identified using MASIGPRO (Conesa *et al.* 2006) in the Bioconductor package with default settings. The two-step regression approach including the least-squares estimation of parameters was performed to construct a general regression model for each OTU, followed by a stepwise regression to select the OTUs with statistically significant stage changes (FDR-corrected  $P$ -values  $< 0.05$ ). The visualization of significant OTUs was based on a cluster analysis for group OTUs sharing a similar profile.

For each treatment, STRs were constructed on the basis of their degree of richness and were then calculated using the moving window (White *et al.* 2006). In brief, a time series was partitioned into as many window subsets as possible based on the number of observations, and the STR model (the power law relationship between time and richness) was fitted for each window. TDRs were estimated by log-linear model fitting between the changes in the community structure (as assessed by pairwise Bray–Curtis dissimilarity) and days elapsed. Community dissimilarities were converted to similarities by subtracting them from 1. Arrhenius (log–log) plots were used for modelling TDRs using the equation  $\ln(S_s) = \text{constant} - w \ln(T)$ , where  $S_s$  is the pairwise similarity in community composition,  $T$  is the time interval and the slope ( $w$ ) is a measure of the rate of community turnover across time (Nekola & White 1999).

The identification of CRT was conducted by following the previously reported procedure (Shade *et al.* 2014). The model detected CRT with a bimodal distribution in the relative abundance of OTUs; it used a threshold for the coefficient of bimodality  $\geq 0.90$  and an abundance threshold of 0.1% when blooming. The partitioned Bray–Curtis dissimilarity between two samples attributable to a subset of the community was calculated as the fraction of beta diversity attributed to the CRT. Only CRT were used to calculate the summation in the numerator of the Bray–Curtis dissimilarity expression, while all of the taxa were used to calculate the scaling summation in the denominator.

Co-occurrence networks were constructed for bacterial communities in the 10 subcultures, and OTUs with an average relative abundance above 0.001% were included in the analysis. Robust correlations were defined as those with Spearman's correlation coefficients that were between two OTUs  $> 0.6$  and  $P$ -values  $< 0.01$ , and they formed the edges, while selected OTUs served as network nodes. Betweenness centrality can discern modules that maintain connectivity in a network and is frequently used to define keystone species within a system (Vick-Majors *et al.* 2014; Banerjee *et al.* 2015). Therefore, the betweenness

centrality values were calculated for each node and compared between CRT and other OTUs using Wilcoxon rank-sum tests.

All statistical analyses were performed in the R environment (<http://www.r-project.org>) using VEGAN (Oksanen *et al.* 2015), LABDSV (Roberts 2007), FDRTOOL (Klaus & Strimmer 2013), IGRAPH (Csardi & Nepusz 2006), HMISC (Harrell Jr 2008), GGPLOT2 (Wickham 2009) and GPLOTS (Warnes *et al.* 2009) packages.

## Results

### *Degradation of pollutants and distribution of taxa in microcosm communities*

In this study, 40 separate pollutant-degrading communities were obtained, corresponding to 10 stages of subculturing for the PHE, C18, PC and PCC treatments. The degradation rates of organic pollutants in these communities were  $> 80\%$  (Fig. S1, Supporting information). In treatment C18, the degradation efficiency of  $n$ -octadecane was almost 100% in every batch, and in the other three treatments, the biodegradation efficiencies tended to increase in successive subcultures, indicating that the pollutant-degrading communities were adapting. In the PCC treatment, the biodegradation of both  $n$ -octadecane and phenanthrene decreased slightly compared with the PC treatment.

The complete sequencing data set from all 40 communities and the original soil sample consisted of 1 225 538 high-quality sequences. The average number of sequences per sample ( $n = 41$ ) was 29 891 (max = 70 838, min = 15 925, and SD = 9738), and the exact numbers were 15 925, 34 114, 25 268, 30 793 and 30 786 for the original soil and for C18, PHE, PC and PCC, respectively. The total number of OTUs was 30 233, of which 99.7% (30 146) were affiliated with the bacterial domain and 0.2% (68) were affiliated with the archaeal domain, while 19 OTUs were unclassified. The original soil sample contained a higher number of OTUs, but a lower number of sequences (Table S1, Supporting information) than all of the enriched communities. At the phylum level, *Proteobacteria* and *Bacteroidetes* were the predominant groups in all 41 communities, with relative abundance in the ranges of 46.6–77.1% and 15.3–34.2%, respectively (Fig. S2, Supporting information). *Actinobacteria* were considerably more abundant in C18 than in other treatments. Differences at the class level were significant between the communities (Fig. S3, Supporting information). *Betaproteobacteria* was the dominant group in PHE, with a relative abundance of 49.4%. *Actinobacteria* (19.6%) and *Sphingobacteria* (11.6%) were the most abundant groups in C18. *Flavobacteria* was the most abundant class in the PCC communities.

### Bacterial patterns associated with pollutants

The CAP based on the weighted UniFrac dissimilarity (Fig. 1A) revealed that different treatments were significant drivers of bacterial beta diversity, and the four treatments formed distinct clusters in the ordination space. PERMANOVA and ANOSIM confirmed the presence of distinct bacterial communities that responded to different treatments (Table 1). Significant taxonomic differences between the treatments were examined using CDA based on genera with a relative abundance of >0.5% (Fig. 1B). In the C18 treatment, *Sphingobacterium*, *Terrimonas*, *Nocardia*, *Azospirillum*, *Gordonia* and *Thermomonas* were the abundant genera, while *Hydrogenophaga*, *Novosphingobium*, *Naxibacter* and *Sphingopyxis* were dominant in the PHE treatment. *Pseudoxanthomonas*, *Parvibaculum*, *Flavobacterium*, *Lactobacillus* and *Enticicia* were abundant genera in the PC treatment, and *Delftia*, *Dokdonella*, *Chryseobacterium*, *Stenotrophomonas* and *Aquabacterium* were dominant in the PCC treatment.

The contributions of different microbial populations to the overall community structure were evaluated using a bipartite association network to visualize the associations between the OTUs and treatments (Fig. 2). For this purpose, we only focused on OTUs that differed significantly among treatments, because their changes were primarily driven by exposure to pollutants. The indicator statistics for 1320 OTUs (average

relative abundance > 0.001%) resulted in the selection of 597 significant OTUs ( $q < 0.05$ ) that were associated with specific treatments. The association strengths (correlation coefficient,  $R$ ) of OTUs ranged from 0.34 to 1.0. In total, 15 clusters of OTUs were generated in the bipartite network. In cluster 1, 37.4% of the indicator OTUs were associated with cross-combinations of all treatments. In clusters 2–11, approximately 53.3% of the OTUs were associated with cross-combinations of two or three treatments. In clusters 12–15, 9.1% of the OTUs were most strongly associated with a single treatment, indicating a separated effect by different pollutants on the microbial communities. The results of the bipartite network showed that large proportions of the indicator OTUs were cross-combinations, indicating that similar taxonomic groups comprised communities from different treatments; however, their abundance differed significantly between treatments.

### Succession patterns of bacterial communities

In general, the differences in the microbial community compositions between treatments increased through progressive phases (from I to III), as demonstrated using PERMANOVA and ANOSIM (Table S2, Supporting information).

Based on the MASIGPRO analysis, OTUs with an average relative abundance >0.001% in all treatments were

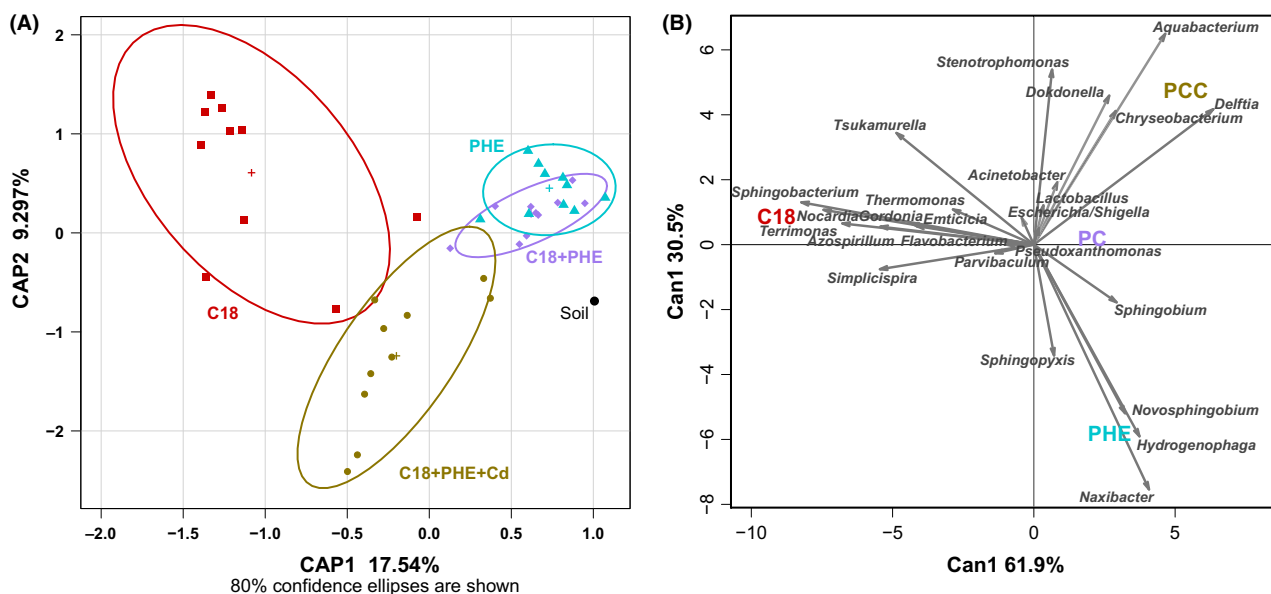


**Fig. 1** Distinct microbial patterns following different treatments. (A) Constrained analysis of the principal coordinates (CAP) of microbial communities among 41 communities from four treatments (C18, *n*-octadecane, '■'; PHE, phenanthrene, '▲'; PC, phenanthrene + *n*-octadecane, '◆'; and PCC, phenanthrene + *n*-octadecane + CdCl<sub>2</sub>, '●') and the original soil based on the weighted UniFrac distance. The 80% confidence ellipses surround each treatment group, '+' represent the centre of the ellipses. (B) Canonical discriminant analysis plot comparing treatments against bacterial taxa loadings based on genera with relative abundance levels > 0.5%. Arrows represent the degree of correlation between each taxon and each treatment as a measure of the predictive discrimination of each treatment. [Colour figure can be viewed at [wileyonlinelibrary.com](http://wileyonlinelibrary.com)]

**Table 1** ANOSIM and PERMANOVA of microbial diversity in microcosms following different pollutant treatments

	Bray–Curtis				Weighted UniFrac			
	ANOSIM		ADONIS		ANOSIM		ADONIS	
	R	P	R <sup>2</sup>	P	R	P	R <sup>2</sup>	P
Treatment*	0.5468	0.001	0.3358	0.001	0.4446	0.001	0.3364	0.001
C18 vs. PHE	0.7247	0.001	0.3047	0.001	0.6807	0.001	0.3540	0.001
C18 vs. PC	0.5376	0.001	0.2189	0.001	0.5869	0.001	0.2641	0.002
C18 vs. PCC	0.5238	0.001	0.2123	0.001	0.4269	0.001	0.2305	0.001
PHE vs. PC	0.3264	0.004	0.1695	0.003	0.2847	0.002	0.1517	0.003
PHE vs. PCC	0.176	0.015	0.1144	0.003	0.2302	0.001	0.1480	0.001
PC vs. PCC	0.468	0.002	0.1994	0.002	0.334	0.001	0.2006	0.001

\*C18 = 500 mg/L *n*-octadecane; PHE = 500 mg/L phenanthrene; PC = 250 mg/L phenanthrene + 250 mg/L *n*-octadecane; and PCC = 250 mg/L phenanthrene + 250 mg/L *n*-octadecane + 50 mg/L CdCl<sub>2</sub>.

classified into three groups; Group 1 (regression) included 601 (total = 1038), 562 (total = 1073), 553 (total = 1125) and 487 (total = 1108) OTUs for which the abundance levels were significantly decreased in successive subculture phases in C18, PHE, PC and PCC treatments, respectively (Fig. 3). Group II (induction) included 254, 271, 227 and 281 OTUs that were significantly increased in successive subculture phases in the four treatments, respectively; and Group III (fluctuation) contained 12, 31, 50 and 3 OTUs that were increased in the second phase and decreased in the third phase in the four treatments, respectively. These results demonstrated a similar dynamic pattern in microbial communities that were subjected to different treatments. There were fewer OTUs smaller in Group III than in Groups I and II, indicating that the dynamic patterns were dominated by *repression* and *induction* rather than *fluctuation*.

To further investigate the effects of the tested pollutants, the top 15 most abundant taxa in Group 2 for each treatment were compared using a heatmap (Fig. S4, Supporting information). These OTUs included diverse taxa in the *Proteobacteria*, *Bacteroidetes*, *Actinobacteria* and *Firmicutes*. In the C18 communities, enriched OTUs were primarily attributed to the genera *Tsukamurella*, *Azospirillum*, *Sphingobacterium*, *Naxibacter* and *Rhodococcus*, whereas *Naxibacter*, *Delftia*, *Rhizobium* and *Lactobacillus* were predominant in the PHE communities. Furthermore, *Acinetobacter*, *Delftia*, *Lactobacillus*, *Flavobacterium* and *Streptophyta* were dominant in the PC treatment, while *Aquabacterium*, *Novosphingobium*, *Pseudomonas* and *Simplicispira* were abundant in the PCC communities. Some enriched OTUs were common in different communities (Fig. S4, Supporting information), demonstrating that similar taxonomic/functional groups might contribute to the degradation of the tested organic pollutants.

### Species–time and time–decay relationships

The accumulation of species richness was estimated by measuring the STRs, which were significant among the four treatments ( $P < 0.05$ ), indicating an increase in the cumulative species richness over time. PHE communities had the lowest STR exponent (0.76), while PC and PCC communities had the highest exponents (0.80); C18 was only slightly lower (0.79). Moreover, significant TDRs were observed in the microbial communities that responded to the four treatments, as estimated by a linear regression from the log-transformed microbial community similarity based on 1 *minus* Bray–Curtis dissimilarity (Fig. 4). The microbial community temporary turnover slopes ( $w$ ) were increased by  $-0.33$  for PHE,  $-0.38$  for PCC,  $-0.51$  for PC and  $-0.59$  for C18. The observation of significant STRs and TDRs strongly indicates the occurrence of microbial community succession during the enrichment process.

### Conditionally rare taxa

Based on the coefficient of the bimodal distribution  $\geq 0.90$  and an abundance threshold of 0.1% when blooming, 116 (1.6% of total OTUs), 41 (0.7%), 57 (0.8%) and 33 (0.6%) OTUs were categorized as CRT in C18, PHE, PC and PCC treatments, respectively. We next explored the temporal dynamics of microbial communities adapting to distinct combinations of pollutants. The presence of highly synchronous CRT in the hierarchical cluster analysis (Fig. S5, Supporting information) indicated similar temporal dynamics in the four treatments. Moreover, the Bray–Curtis dissimilarity between CRT and the whole community was strongly correlated (the correlation coefficients ranged from 0.61 to 0.92,  $P < 0.001$ ) for all treatments, as demonstrated using the Mantel test (Pearson method, 9999 permutations). Based

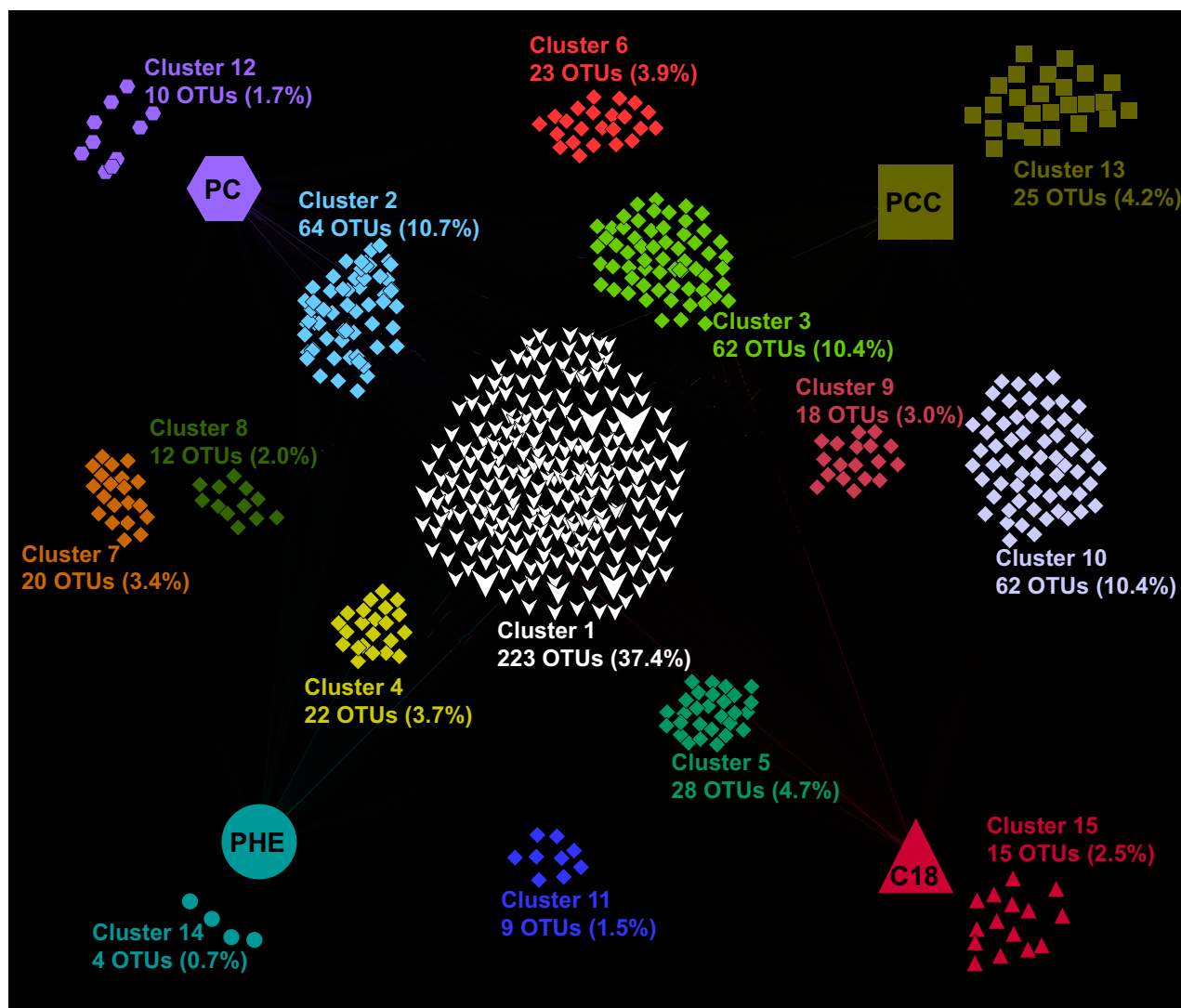


Fig. 2 Bipartite association network showing positive associations between different treatments (C18, *n*-octadecane; PHE, phenanthrene; PC, phenanthrene + *n*-octadecane; and PCC, phenanthrene + *n*-octadecane + CdCl<sub>2</sub>) and significantly associated operational taxonomic units (OTUs). Node sizes represent the relative abundance levels of OTUs. Edges represent the association patterns of individual OTUs with treatments. Diamond-shaped nodes represent OTUs that were associated with two or three treatments. White nodes represent cross-combination OTUs associated with all treatments. The number of OTUs and relative abundance levels are provided for each cluster. [Colour figure can be viewed at [wileyonlinelibrary.com](http://wileyonlinelibrary.com)]

on the Bray–Curtis dissimilarity (Fig. S6, Supporting information), the CRT accounted for a considerable fraction of the community dissimilarity in different communities (16.1% in C18, 10.5% in PHE, 26.9% in PC and 26.4% in PCC), despite the relatively low proportion of OTUs (0.6–1.6%).

Most CRT were treatment-specific (Fig. S7, Supporting information) and were assigned to *Proteobacteria*, *Bacteroidetes*, *Actinobacteria* and *Firmicutes*, indicating their broad range of phylogenetic diversity. At the class level, the CRT were distinct in different communities (Fig. S8, Supporting information). CRT from C18 were the most diverse, belonging to 16 classes that were

dominated by *Actinobacteria*, *Gammaproteobacteria*, *Sphingobacteria* and *Betaproteobacteria*. Most CRT were affiliated with *Betaproteobacteria* and *Gammaproteobacteria* in the PHE communities. *Gammaproteobacteria* dominated CRT in the PC treatment. Both *Gammaproteobacteria* and *Flavobacteria* were abundant in the PCC treatment.

The co-occurrence networks for different treatments, which were based on correlations between OTUs (average relative abundance > 0.001%), revealed the major topological feature of the CRT. The resulting networks consisted of 3181, 3262, 3368 and 3053 nodes with 326 160, 254 368, 314 375 and 265 919 edges for C18, PHE, PC and PCC, respectively. The betweenness

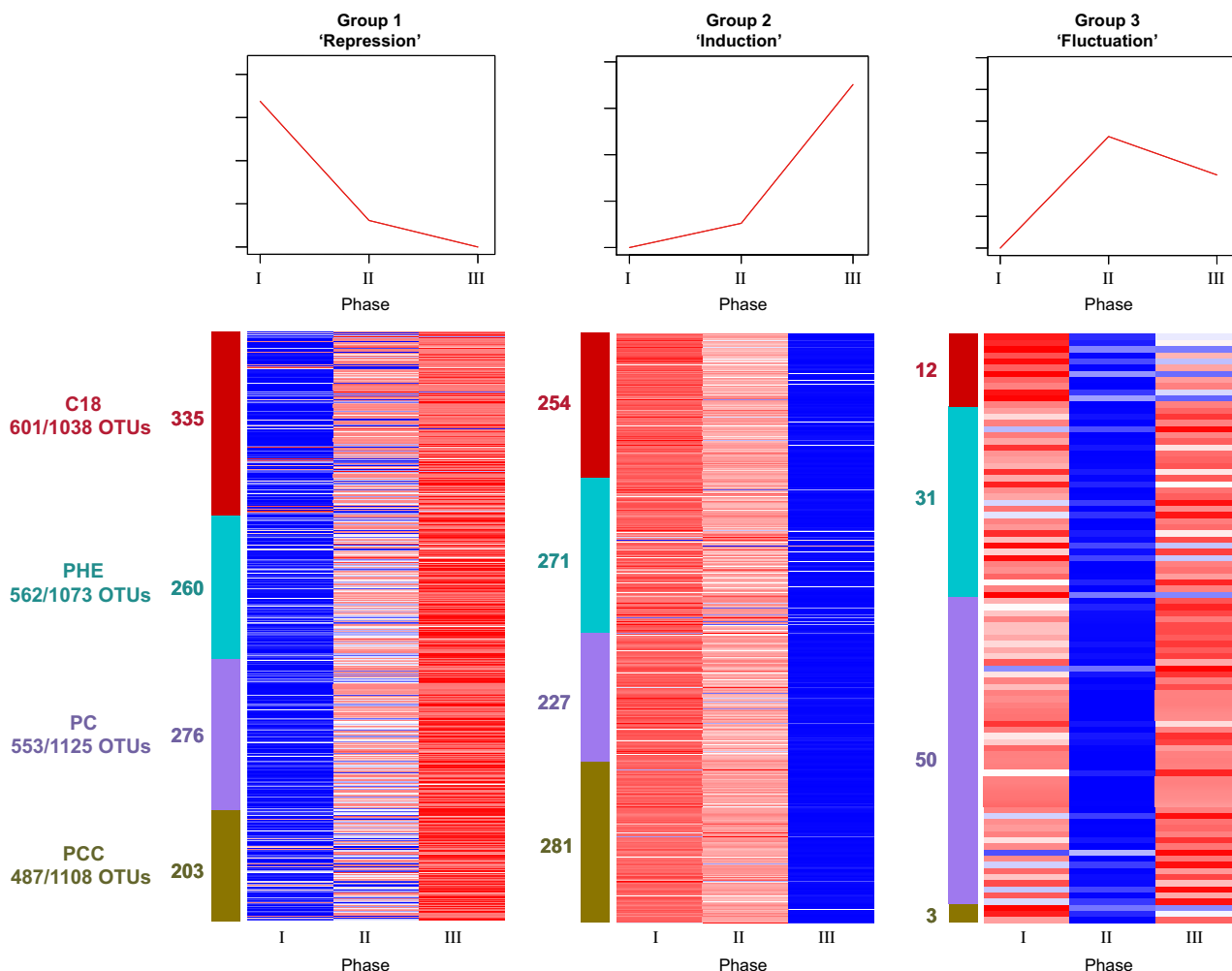


**Fig. 3** Temporal dynamic patterns of microbial communities during three enrichment phases (I, subcultures 1–3; II, subcultures 4–7; and III, subcultures 8–10) that were determined using the maSigPro method. Based on OTUs with an average relative abundance >0.001%, the number of significant operational taxonomic units (OTUs) and total OTUs is provided for each treatment. Temporal dynamic visualization of significant OTUs is based on cluster analysis for grouping OTUs with similar profiles (displayed as heatmaps). Each row in the heatmap has been standardized to have a mean of zero and a standard deviation of one. The intensity of the colour in the heatmap is proportional to the standardized relative abundance of the taxa. The number of significant OTUs for each cluster is provided for each treatment. [Colour figure can be viewed at [wileyonlinelibrary.com](http://wileyonlinelibrary.com)]

centrality values of the nodes belonging to CRT were significantly higher than those of other nodes (Fig. 5), suggesting that CRT were more likely located in core and central positions within the networks of all treatment communities.

## Discussion

Elucidating the mechanisms of microbial succession is a major goal in the field of microbial ecology. The results of the analyses that were performed in the present study revealed similar dynamic patterns in bacterial communities that responded to different pollutants. The studied communities displayed higher rates of occurrence in terms of new taxa and temporal turnover than

the rates reported in other studies of microbial communities in air, water and soil samples (Shade *et al.* 2013). This suggests that the repeated addition of pollutants accelerated microbial succession in the tightly controlled microcosms. CRT from distinct communities occupied central positions in the networks and revealed a treatment-specific response to individual or combined pollutants.

### *Temporal dynamic patterns of microbial taxa in response to pollutants*

Pollutants can have a large influence on the microbial community structure, and microorganisms are often able to respond rapidly to environmental changes

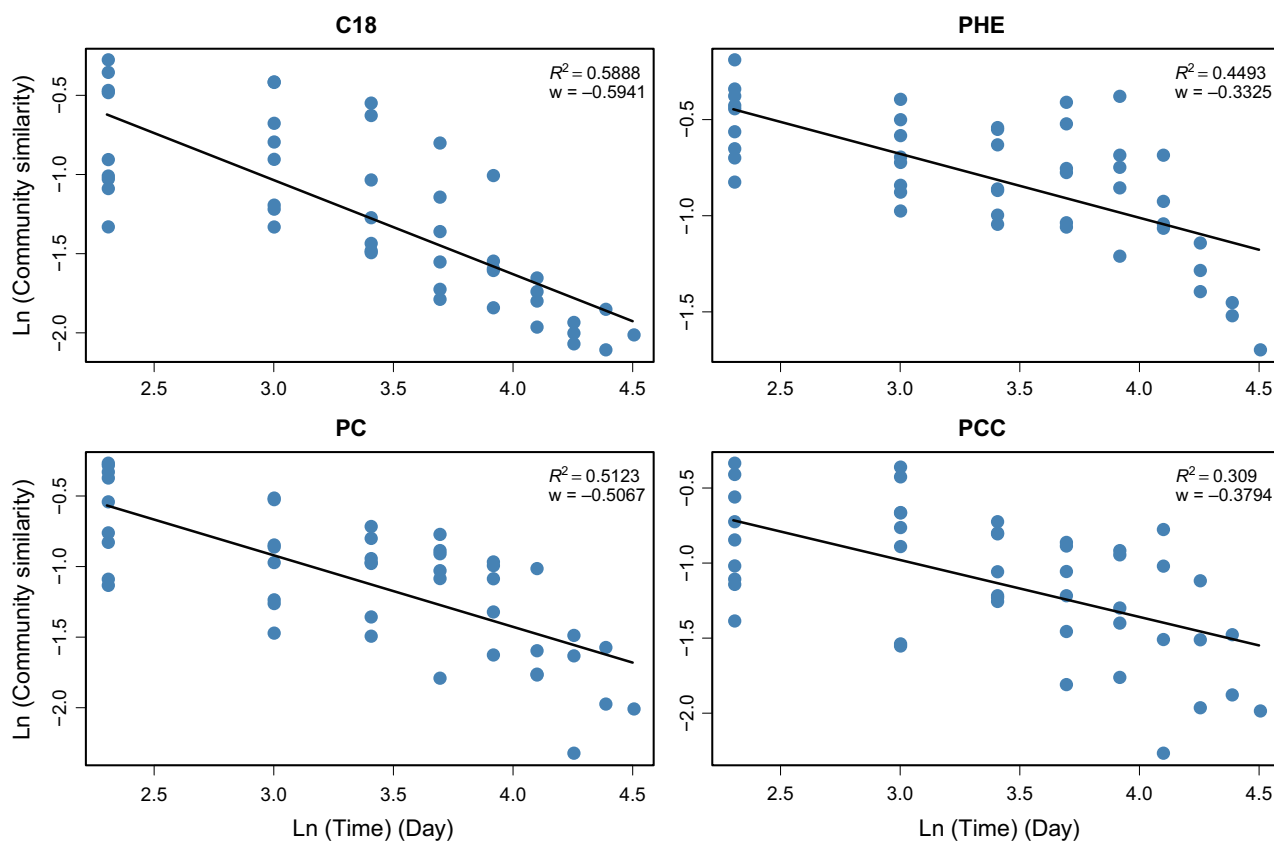


Fig. 4 Time-decay curves for microbial communities in the four treatments (C18, *n*-octadecane; PHE, phenanthrene; PC, phenanthrene + *n*-octadecane; and PCC, phenanthrene + *n*-octadecane + CdCl<sub>2</sub>). The line represents the log-linear time-decay model. The slope ( $w$ ) and fitting degree ( $R^2$ ) of the line are provided. [Colour figure can be viewed at [wileyonlinelibrary.com](http://wileyonlinelibrary.com)]

(Singh *et al.* 2010; Jiao *et al.* 2016). In the present study, the organic pollutants *n*-octadecane and phenanthrene served as the sole energy and carbon sources for chemoheterotrophs in the microcosms, while the heavy metal Cd (in the form of CdCl<sub>2</sub>) functioned as an environmental stressor that promoted selection. Dynamic patterns in the microbial communities during enrichment were explored using MASIGPRO and were similar in communities that responded to different pollutants (Fig. 3). Specifically, *repression* and *induction* dominated, while *fluctuation* was not significant during the enrichment. These findings could be explained by the selection of microorganisms with a potentially high growth rate and the elimination of those without the capacity to adapt as quickly (Viñas *et al.* 2005).

In particular, OTUs associated with *induction* may be strongly associated with pollutant degradation, because these OTUs were increased in terms of relative abundance during enrichment. The dominant enriched OTUs in the *Tsukamurella*, *Azospirillum* and *Sphingobacterium* genera in the C18 communities might correlate with their capacity to degrade hexadecane (for *Tsukamurella*; Tebyanian *et al.* 2013) or alkane (for *Azospirillum* and

*Sphingobacterium*; Gałazka *et al.* 2012; Giebler *et al.* 2013). The enriched genera *Delftia*, *Lactobacillus*, *Acinetobacter*, *Flavobacterium* and *Streptophyta* in the PHE and PC communities have previously been associated with hydrocarbon degradation (Pichrtová *et al.* 2013; Atlas *et al.* 2015; Shao *et al.* 2015; Wu *et al.* 2016). Meanwhile, *Aquabacterium*, *Novosphingobium*, *Pseudomonas* and *Simplicispira* were enriched in communities that were exposed to CdCl<sub>2</sub>, indicating possible roles in combined hydrocarbon degradation and metal tolerance, especially because the former three genera were previously identified as hydrocarbon degraders (Masuda *et al.* 2014; Xia *et al.* 2014; Yun *et al.* 2014). Interestingly, even though the initial inoculum used in the present study was collected at a site that was ~360 km away from where the inoculum was collected for our previous study (Jiao *et al.* 2016), many of the bacterial genera were similar. This finding suggests that similar organic pollutants may select similar bacterial degraders in different soils, as the physicochemical properties of the soils in the two studies were quite different.

The MASIGPRO method is usually used with microarray or RNA-seq data to identify differential expression

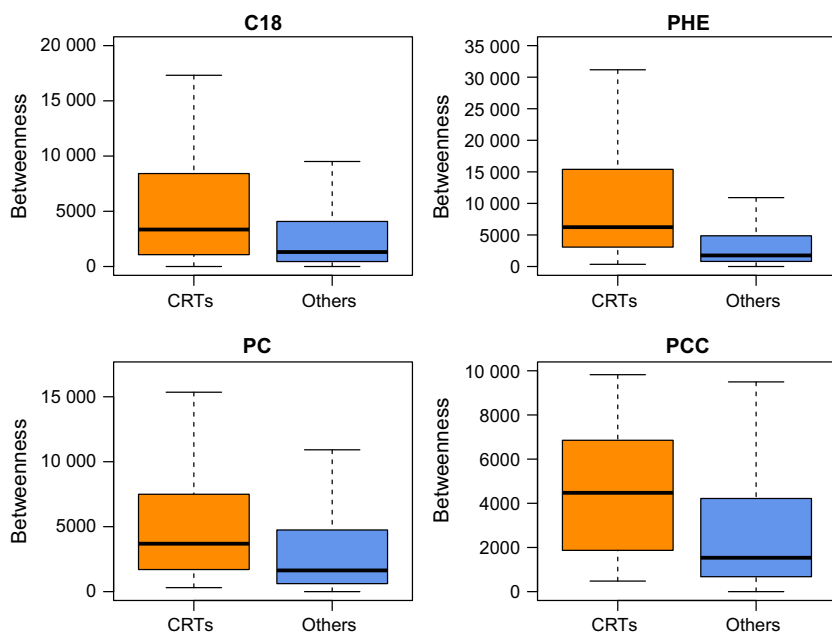


**Fig. 5** Comparison of the betweenness centrality values between conditionally rare taxa (CRT) and other operational taxonomic units (Others) in the four treatments (C18, *n*-octadecane; PHE, phenanthrene; PC, phenanthrene + *n*-octadecane; and PCC, phenanthrene + *n*-octadecane + CdCl<sub>2</sub>). The values were significantly different between the two groups on the basis of a Wilcoxon rank-sum test ( $P < 0.05$ ). [Colour figure can be viewed at [wileyonlinelibrary.com](http://wileyonlinelibrary.com)]

profiles in time-course experiments (Díaz-Gimeno *et al.* 2011; Nueda *et al.* 2014). Our results showed that MASIG-PRO could also reveal the dynamic patterns of microbial communities based on 16S rRNA gene metagenomic data.

#### *Characteristics of newly selected taxa and the microbial turnover rate*

Species–time relationship and TDR have frequently been used to probe plant and animal communities (Preston 1960; McNaughton 1977; Ives *et al.* 2003; Ives & Carpenter 2007) and to analyse microbial succession in microcosm communities (Shade *et al.* 2013). The STR exponent can give an indication of the rate at which new taxa are observed in a community over time, and a higher exponent indicates that a greater number of newly introduced taxa are present (Preston 1960). In our study, the tightly controlled microcosms provided a closed environment; hence, new taxa could not be introduced through dispersal. We speculate that the newly detected taxa may be derived from taxa that are present at low levels in the original inoculum. A previous study demonstrated that the vast majority of taxa in an ecosystem remain present at all times, but their proportions may vary. Variations in community composition are due to changes in the relative abundance of taxa, rather than extinction and recolonization (Caporaso *et al.* 2012). An STR exponent between 0.76 and 0.80 suggested that more new detected taxa appeared in the communities as the enrichment process advanced. For comparison, STR exponents from microbial

communities that were grown in a suite of nonpolluted habitats, including air, seawater, flowers, soil and freshwater, ranged from 0.24 to 0.61 (Shade *et al.* 2013). The rate of newly detected taxa in the enriched microcosms was clearly higher compared with the natural environment.

To confirm this observation, the STRs of microbial communities in the microcosms were estimated using data from our previous study (Jiao *et al.* 2016), which involved a similar experimental design, but with different soil samples. Specifically, the physicochemical properties of the two soil samples were very different, especially the degrees of contamination (data not shown). The STRs for these microcosms in our previous study were also significant, with exponents ranging from 0.72 to 0.77, verifying the observation described above. The higher rate of newly identified detected taxa in the enriched microcosms could be due to the fluctuating abiotic conditions during the degradation of the organic pollutants (Shade *et al.* 2013). Based on these results, we speculate that the higher rate of newly detected taxa over time may alter the balance of microbial ecosystems in soils that are continually polluted with oil or other organic pollutants.

Time–decay relationships also provide information on community succession dynamics, and temporary turnover slopes ( $w$ ) estimate the rate of temporal change in community structure. A community with a slope of zero does not change over time, whereas a more negative slope indicates a faster rate of community temporal turnover (Nekola & White 1999). In our study, the TDRs were significant for microbial communities in all

treatments. A temporal decay in community similarity underlies key ecological principles and appears to be universal in microbial ecosystems (Korhonen *et al.* 2010; Gonzalez *et al.* 2012). In previous studies, the turnover slopes in the air, seawater, flowers, soil and freshwater habitats from temporal scales of 1 day to 6 years ranged between 0 and  $-0.3$  (Oliver *et al.* 2012; Hatosy *et al.* 2013; Liang *et al.* 2015). The much greater turnover slopes in the present study ( $-0.33$  to  $-0.59$ ) indicate the rapid elimination and replacement of species through selection in response to different pollutants.

Our previous analysis of TDRs for the microbial communities in the microcosms (Jiao *et al.* 2016) indicated that they were also significant, with turnover slopes ranging from  $-0.31$  to  $-0.57$  (Fig. S9, Supporting information). This finding provides further evidence that turnover slopes are higher in microcosms than in natural habitats. The possible reasons for this difference are as follows: (i) the closed microcosm systems ensured that the pollutants could directly affect microbial population dynamics without disturbance from other environmental factors (Viñas *et al.* 2005) and (ii) the repeated introduction of pollutants placed a persistent selection pressure on the communities, and they accelerated the elimination and replacement of less adaptable species; this resulted in a rapid re-equilibration of the microbial community in which the members that could adapt quickly thrived. Future work should be conducted in natural habitats to understand the effect of the repeated introduction of pollutants on microbial succession in more complex environments.

#### *Conditionally rare taxa reveal a treatment-specific response and central locations in the network*

Rare microorganisms are receiving increased attention because they have ecologically important roles in ensuring microbial diversity, in that they function as keystone species in microbial communities and mediate biogeochemical processes (Galand *et al.* 2009; Jones & Lennon 2010; Pester *et al.* 2010; Sauret *et al.* 2014). The detection of CRT may facilitate the identification of rare taxa that play potentially critical ecological roles under certain conditions (Shade *et al.* 2014). In the present study, we detected CRT in different communities, and we observed similar lineages between subsets of CRT (Fig. S8, Supporting information) and the entire community (Fig. S3, Supporting information). For example, *Gammaproteobacteria* were abundant in all CRT subsets and in all communities. In PHE communities, *Betaproteobacteria* was the dominant group, and *Flavobacteria* was the most abundant in PCC communities. Therefore, the observed distribution of CRT in communities that

responded to different pollutants indicated a treatment-specific response. This finding suggests that rare but adaptable taxa may thrive under particular conditions following a strong selection pressure and species sorting in response to different pollutants. Additionally, CRT contributed substantially to the temporal variability of different communities. The variation in the dominant taxa determined a large fraction of the community dissimilarity. Taxa capable of 'booming and busting' (CRT) occur widely and contribute to the microbial community dynamics as they are able to expand rapidly under certain conditions (Shade *et al.* 2014). Thus, our results suggest that some rare microorganisms can effectively act as seed banks, while their population densities are largely driven by environmental conditions, rather than the episodic growth of opportunists.

In co-occurrence network analysis, betweenness centrality is a topological feature that represents the potential of an individual node to influence interactions between other nodes in the network (Greenblum *et al.* 2012). A high betweenness centrality value indicates a core and central location in the network, whereas a low betweenness centrality value indicates a more peripheral location (Ma *et al.* 2016). In our study, nodes belonging to CRT consistently displayed higher betweenness centrality values than other nodes. This finding suggests that CRT occupied core and central positions, and they had a pronounced influence on other interactions in the microbial networks. According to a previous study on CRT from different environments, including air, seawater, freshwater and brewery wastewater, some CRT may be indicators of environmental change that can be used to identify the physical, chemical or biological drivers of microbial dynamics (Shade *et al.* 2014). Therefore, the results of the present study suggest that rare taxa may be capable of thriving when provided with suitable conditions, and they may play vital roles in regulating microbial interactions in response to environmental changes.

#### **Conclusions**

In the present study, we investigated the temporal dynamic patterns of microbial communities that responded to pollutants in microcosms. Similar dynamic patterns were observed for bacterial communities responding to different pollutants, and repression and induction dominated the dynamic patterns during enrichment. High rates of newly detected taxa and microbial temporal turnover in microcosms indicated a high rate of microbial succession during enrichment. Additionally, CRT from distinct communities revealed treatment-specific responses to individual or combined

pollutants, and they suggested that initially rare taxa might play vital roles in regulating microbial interactions in response to environmental changes. The functional succession associated with microbial community dynamics in response to pollutants should be further investigated.

## Acknowledgements

This work was funded by the National Science Foundation of China (31270529) and the Cheung Kong Scholars Programme (T2014208). We thank Professor Entao Wang for discussions about the manuscript.

## Conflict of interest

The authors declare no conflicts of interest.

## References

- Anderson MJ (2001) A new method for non-parametric multivariate analysis of variance. *Austral Ecology*, **26**, 32–46.
- Atlas RM, Stoeckel DM, Faith SA, Minard-Smith A, Thorn JR, Benotti MJ (2015) Oil biodegradation and oil-degrading microbial populations in marsh sediments impacted by oil from the deepwater horizon well blowout. *Environmental Science & Technology*, **49**, 8356–8366.
- Banerjee S, Baah-Acheamfour M, Carlyle CN *et al.* (2015) Determinants of bacterial communities in Canadian agroforestry systems. *Environmental Microbiology*, **18**, 1805–1816.
- Brown SP, Jumpponen A (2014) Contrasting primary successional trajectories of fungi and bacteria in retreating glacier soils. *Molecular Ecology*, **23**, 481–497.
- Cáceres MD, Legendre P (2009) Associations between species and groups of sites: indices and statistical inference. *Ecology*, **90**, 3566–3574.
- Caporaso JG, Paszkiewicz K, Field D, Knight R, Gilbert JA (2012) The Western English Channel contains a persistent microbial seed bank. *ISME Journal*, **6**, 1089–1093.
- Clarke KR (1993) Non-parametric multivariate analyses of changes in community structure. *Australian Journal of Ecology*, **18**, 117–143.
- Conesa A, Nueda MJ, Ferrer A, Talón M (2006) maSigPro: a method to identify significantly differential expression profiles in time-course microarray experiments. *Bioinformatics*, **22**, 1096–1102.
- Csardi G, Nepusz T (2006) The igraph software package for complex network research. *InterJournal Complex Systems*, **1695**, 1–9.
- Díaz-Gimeno P, Horcajadas JA, Martínez-Conejero JA *et al.* (2011) A genomic diagnostic tool for human endometrial receptivity based on the transcriptomic signature. *Fertility and Sterility*, **95**, 50–60. e15.
- Eiler A, Heinrich F, Bertilsson S (2012) Coherent dynamics and association networks among lake bacterioplankton taxa. *ISME Journal*, **6**, 330–342.
- Falkowski PG, Fenchel T, Delong EF (2008) The microbial engines that drive Earth's biogeochemical cycles. *Science*, **320**, 1034–1039.
- Fierer N, Nemergut D, Knight R, Craine JM (2010) Changes through time: integrating microorganisms into the study of succession. *Research in Microbiology*, **161**, 635–642.
- Galand PE, Casamayor EO, Kirchman DL, Lovejoy C (2009) Ecology of the rare microbial biosphere of the Arctic Ocean. *Proceedings of the National Academy of Sciences of the United States of America*, **106**, 22427–22432.
- Gałazka A, Król M, Perzyński A (2012) The efficiency of rhizosphere bioremediation with *Azospirillum* sp. and *Pseudomonas stutzeri* in soils freshly contaminated with PAHs and diesel fuel. *Polish Journal of Environmental Studies*, **21**, 345–353.
- van der Gast CJ, Ager D, Lilley AK (2008) Temporal scaling of bacterial taxa is influenced by both stochastic and deterministic ecological factors. *Environmental Microbiology*, **10**, 1411–1418.
- Giebler J, Wick LY, Chatzinotas A, Harms H (2013) Alkane-degrading bacteria at the soil–litter interface: comparing isolates with T-RFLP-based community profiles. *FEMS Microbiology Ecology*, **86**, 45–58.
- Gilbert JA, Steele JA, Caporaso JG *et al.* (2012) Defining seasonal marine microbial community dynamics. *ISME Journal*, **6**, 298–308.
- Gonzalez A, King A, Robeson II MS *et al.* (2012) Characterizing microbial communities through space and time. *Current Opinion in Biotechnology*, **23**, 431–436.
- Greenblum S, Turnbaugh PJ, Borenstein E (2012) Metagenomic systems biology of the human gut microbiome reveals topological shifts associated with obesity and inflammatory bowel disease. *Proceedings of the National Academy of Sciences of the United States of America*, **109**, 594–599.
- Harrell Jr FE (2008) *Hmisc: harrell miscellaneous*, R package version 3, 4-4. Available from <http://CRAN.r-project.org/package=Hmisc>.
- Hatosy SM, Martiny JB, Sachdeva R, Steele J, Fuhrman JA, Martiny AC (2013) Beta diversity of marine bacteria depends on temporal scale. *Ecology*, **94**, 1898–1904.
- Horz H-P, Conrads G (2010) The discussion goes on: what is the role of Euryarchaeota in humans? *Archaea*, **2010**, 1–8.
- Huesemann MH (1995) Predictive model for estimating the extent of petroleum hydrocarbon biodegradation in contaminated soils. *Environmental Science & Technology*, **29**, 7–18.
- Hur M, Kim Y, Song HR, Kim JM, Im Choi Y, Yi H (2011) Effect of genetically modified poplars on soil microbial communities during the phytoremediation of waste mine tailings. *Applied and Environmental Microbiology*, **77**, 7611–7619.
- Ives AR, Carpenter SR (2007) Stability and diversity of ecosystems. *Science*, **317**, 58–62.
- Ives A, Dennis B, Cottingham K, Carpenter S (2003) Estimating community stability and ecological interactions from time-series data. *Ecological Monographs*, **73**, 301–330.
- Jiao S, Chen W, Wang E *et al.* (2016) Microbial succession in response to pollutants in batch-enrichment culture. *Scientific Reports*, **6**, 21791.
- Jones SE, Lennon JT (2010) Dormancy contributes to the maintenance of microbial diversity. *Proceedings of the National Academy of Sciences of the United States of America*, **107**, 5881–5886.
- Klaus B, Strimmer K (2013) *fdrtool: Estimation of (local) False Discovery Rates and Higher Criticism*, R package version 3. <http://CRAN.R-project.org/package=fdrtool>.
- Koenig JE, Spor A, Scalfone N *et al.* (2011) Succession of microbial consortia in the developing infant gut microbiome.

- Proceedings of the National Academy of Sciences of the United States of America*, **108**, 4578–4585.
- Korhonen JJ, Soininen J, Hillebrand H (2010) A quantitative analysis of temporal turnover in aquatic species assemblages across ecosystems. *Ecology*, **91**, 508–517.
- LaRoche J, Breitbart E (2005) Importance of the diazotrophs as a source of new nitrogen in the ocean. *Journal of Sea Research*, **53**, 67–91.
- Leininger S, Urich T, Schlöter M *et al.* (2006) Archaea predominate among ammonia-oxidizing prokaryotes in soils. *Nature*, **442**, 806–809.
- Liang Y, Jiang Y, Wang F *et al.* (2015) Long-term soil transplant simulating climate change with latitude significantly alters microbial temporal turnover. *ISME Journal*, **9**, 2561–2572.
- Ma B, Wang H, Dsouza M *et al.* (2016) Geographic patterns of co-occurrence network topological features for soil microbiota at continental scale in eastern China. *ISME Journal*, **10**, 1891–1901.
- MacArthur RH, Wilson EO (2015) *Theory of Island Biogeography (MPB-1)*. Princeton University Press, Princeton, New Jersey.
- Masuda H, Shiwa Y, Yoshikawa H, Zylstra GJ (2014) Draft genome sequence of the versatile alkane-degrading bacterium *Aquabacterium* sp. strain NJ1. *Genome Announcements*, **2**, e01271–01214.
- McNaughton SJ (1977) Diversity and stability of ecological communities: a comment on the role of empiricism in ecology. *The American Naturalist*, **111**, 515–525.
- Mikkonen A, Lappi K, Wallenius K, Lindström K, Suominen L (2011) Ecological inference on bacterial succession using curve-based community fingerprint data analysis, demonstrated with rhizoremediation experiment. *FEMS Microbiology Ecology*, **78**, 604–616.
- Nekola JC, White PS (1999) The distance decay of similarity in biogeography and ecology. *Journal of Biogeography*, **26**, 867–878.
- Nueda MJ, Tarazona S, Conesa A (2014) Next maSigPro: updating maSigPro bioconductor package for RNA-seq time series. *Bioinformatics*, **30**, 2598–2602.
- Oksanen J, Blanchet FG, Kindt R *et al.* (2015) *vegan: Community Ecology Package*. R package version 2.2-1. Available from <http://CRAN.r-project.org/package=vegan>.
- Oliver A, Lilley AK, van der Gast CJ (2012) *Species-Time Relationships for Bacteria*. Horizon Scientific Press, Norwich, UK.
- Pester M, Bittner N, Deevong P, Wagner M, Loy A (2010) A 'rare biosphere' microorganism contributes to sulfate reduction in a peatland. *ISME Journal*, **4**, 1591–1602.
- Pichtová M, Remias D, Lewis LA, Holzinger A (2013) Changes in phenolic compounds and cellular ultrastructure of Arctic and Antarctic strains of *Zygnema* (Zygnematophyceae, Streptophyta) after exposure to experimentally enhanced UV to PAR ratio. *Microbial Ecology*, **65**, 68–83.
- Preston FW (1960) Time and space and the variation of species. *Ecology*, **41**, 611–627.
- Redford AJ, Fierer N (2009) Bacterial succession on the leaf surface: a novel system for studying successional dynamics. *Microbial Ecology*, **58**, 189–198.
- Roberts D (2007) *labdsv: Ordination and Multivariate Analysis for Ecology*, R package version 1. Available from <http://CRAN.r-project.org/package=labdsv>.
- Rosenzweig ML (1995) *Species Diversity in Space and Time*. Cambridge University Press, Cambridge.
- Sauret C, Séverin T, Vétion G *et al.* (2014) 'Rare biosphere' bacteria as key phenanthrene degraders in coastal seawaters. *Environmental Pollution*, **194**, 246–253.
- Shade A, Caporaso JG, Handelsman J, Knight R, Fierer N (2013) A meta-analysis of changes in bacterial and archaeal communities with time. *ISME Journal*, **7**, 1493–1506.
- Shade A, Jones SE, Caporaso JG *et al.* (2014) Conditionally rare taxa disproportionately contribute to temporal changes in microbial diversity. *MBio*, **5**, e01371–01314.
- Shao Y, Wang Y, Wu X *et al.* (2015) Biodegradation of PAHs by *Acinetobacter* isolated from karst groundwater in a coal-mining area. *Environmental Earth Sciences*, **73**, 7479–7488.
- Singh BK, Bardgett RD, Smith P, Reay DS (2010) Microorganisms and climate change: terrestrial feedbacks and mitigation options. *Nature Reviews Microbiology*, **8**, 779–790.
- Smoot ME, Ono K, Ruschinski J, Wang P-L, Ideker T (2011) Cytoscape 2.8: new features for data integration and network visualization. *Bioinformatics*, **27**, 431–432.
- Storey JD (2002) A direct approach to false discovery rates. *Journal of the Royal Statistical Society: Series B (Statistical Methodology)*, **64**, 479–498.
- Tebyanian H, Hassanshahian M, Kariminik A (2013) Hexadecane-degradation by *Teskumurella* and *Stenotrophomonas* strains isolated from hydrocarbon contaminated soils. *Jundishapur Journal of Microbiology*, **6**, e9182.
- Thavamani P, Megharaj M, Naidu R (2012) Multivariate analysis of mixed contaminants (PAHs and heavy metals) at manufactured gas plant site soils. *Environmental Monitoring and Assessment*, **184**, 3875–3885.
- Vick-Majors TJ, Priscu JC, Amaral-Zettler LA (2014) Modular community structure suggests metabolic plasticity during the transition to polar night in ice-covered Antarctic lakes. *ISME Journal*, **8**, 778–789.
- Viñas M, Sabaté J, Guasp C, Lalucat J, Solanas AM (2005) Culture-dependent and-independent approaches establish the complexity of a PAH-degrading microbial consortium. *Canadian Journal of Microbiology*, **51**, 897–909.
- Warnes GR, Bolker B, Bonebakker L *et al.* (2009) *gplots: Various R Programming Tools for Plotting Data*, R package version 2. Available from <http://CRAN.r-project.org/package=gplots>.
- White EP, Adler PB, Lauenroth WK *et al.* (2006) A comparison of the species–time relationship across ecosystems and taxonomic groups. *Oikos*, **112**, 185–195.
- Wickham H (2009) *ggplot2: Elegant Graphics for Data Analysis*. Springer Science & Business Media, Dordrecht.
- Wilson K (1987) Preparation of genomic DNA from bacteria. In: *Current Protocols in Molecular Biology*. (eds Ausubel FM, Brent R, Kingston RE, Moore DD, Seidman JG, Smith JA, Struhl K), pp. 241–245. John Wiley & Sons, Inc, New York.
- Wu W, Huang H, Ling Z *et al.* (2016) Genome sequencing reveals mechanisms for heavy metal resistance and polycyclic aromatic hydrocarbon degradation in *Delftia lacustris* strain LZ-C. *Ecotoxicology*, **25**, 234–247.
- Xia W, Du Z, Cui Q *et al.* (2014) Biosurfactant produced by novel *Pseudomonas* sp. WJ6 with biodegradation of *n*-alkanes and polycyclic aromatic hydrocarbons. *Journal of Hazardous Materials*, **276**, 489–498.
- Yu S, Li S, Tang Y, Wu X (2011) Succession of bacterial community along with the removal of heavy crude oil pollutants by multiple biostimulation treatments in the Yellow

River Delta, China. *Journal of Environmental Sciences*, **23**, 1533–1543.

Yu X, Yang J, Wang E, Li B, Yuan H (2015) Effects of growth stage and fulvic acid on the diversity and dynamics of endophytic bacterial community in *Stevia rebaudiana* Bertoni leaves. *Frontiers in Microbiology*, **6**, 867.

Yun SH, Choi CW, Lee SY *et al.* (2014) Proteomic characterization of plasmid pLA1 for biodegradation of polycyclic aromatic hydrocarbons in the marine bacterium, *Novosphingobium Pentaromaticivorans* US6-1. *PLoS One*, **9**, e90812.

All authors contributed intellectual input and assistance to this study and the manuscript preparation. S.J., G.W. and W.C. developed the original framework. S.J. collected the samples. S.J. did data analysis and wrote the paper with help from W.C. and Z.Z.

### Data accessibility

The 16S rRNA Illumina libraries that were obtained from the sequencing company were deposited in the NCBI small read archive (SRA) data set under the study number SRP076750 with the run number SRR3714933–SRR3714936.

### Supporting information

Additional supporting information may be found in the online version of this article.

**Table S1** Microbial alpha-diversity characteristics for enriched consortia and original soil.

**Table S2** ANOSIM and PERMANOVA analysis of microbial diversity during three subculturing phases of different treatments.

**Fig. S1** Degradation rate of *n*-octadecane and phenanthrene in the four treatments at 10 stages.

**Fig. S2** Average relative abundance of phyla in consortia following different treatments and in the original soil sample.

**Fig. S3** Relative abundance of classes in consortia following different treatments and in the original soil sample (Soil, untreated control; C18, *n*-octadecane; PHE, phenanthrene; PC, phenanthrene + *n*-octadecane; and PCC, phenanthrene + *n*-octadecane + CdCl<sub>2</sub>).

**Fig. S4** Heatmap of the relative abundance of the 15 most abundant OTUs responding to different treatments in group 2 of Fig. 3.

**Fig. S5** Hierarchical clustering and heatmap analysis based on the relative abundance of conditionally rare taxa (CRTs) during different subculturing stages in four treatments (C18, *n*-octadecane; PHE, phenanthrene; PC, phenanthrene + *n*-octadecane; and PCC, phenanthrene + *n*-octadecane + CdCl<sub>2</sub>).

**Fig. S6** The contributions of CRTs to entire community beta-diversity responding to different treatments (C18, *n*-octadecane; PHE, phenanthrene; PC, phenanthrene + *n*-octadecane; and PCC, phenanthrene + *n*-octadecane + CdCl<sub>2</sub>) based on Bray-Curtis dissimilarity.

**Fig. S7** Venn diagram of conditionally rare taxa responding to different treatments (C18, *n*-octadecane; PHE, phenanthrene; PC, phenanthrene + *n*-octadecane; and PCC, phenanthrene + *n*-octadecane + CdCl<sub>2</sub>).

**Fig. S8** Taxonomic distribution at the class level of conditionally rare taxa (CRTs) responding to different treatments (C18, *n*-octadecane; PHE, phenanthrene; PC, phenanthrene + *n*-octadecane; and PCC, phenanthrene + *n*-octadecane + CdCl<sub>2</sub>).

**Fig. S9** Time-decay curves for microbial communities in the four treatments based on the data of our previous study (C18, *n*-octadecane; PHE, phenanthrene; PC, phenanthrene + *n*-octadecane; and PCC, phenanthrene + *n*-octadecane + CdCl<sub>2</sub>).